Int J Clin Exp Pathol 2016;9(8):8102-8111
www.ijcep.com /ISSN:1936-2625/IJCEP0025337

Original Article

Morphologic alterations of ovarian malignant Brenner tumors following chemotherapy

Cheol Keun Park[1], Chang Won Koh[2], Gun Yoon[3], Nam Hoon Cho[1], Hyun-Soo Kim[1]

[1]Department of Pathology, Severance Hospital, Yonsei University College of Medicine, Seoul, Republic of Korea; [2]Department of Obstetrics and Gynecology, Seoul National University Hospital, Seoul, Republic of Korea; [3]Department of Obstetrics and Gynecology, Shinsegae Women's Hospital, Daegu, Republic of Korea

Received January 31, 2016; Accepted June 24, 2016; Epub August 1, 2016; Published August 15, 2016

Abstract: Interval debulking surgery following neoadjuvant chemotherapy has become an alternative management for patients with advanced ovarian cancer. However, chemotherapy-induced alterations in cellular morphology may cause diagnostic difficulties for pathologists and inappropriate management by clinicians. We investigated the cytomorphological changes produced by chemotherapy in cytologic and tissue specimens of ovarian malignant Brenner tumors (MBTs). To the best of our knowledge, no data are available on the effect of chemotherapy on MBT cytomorphology. We analyzed cytological and histopathological features of MBT using scraping cytologic preparations, routine hematoxylin and eosin staining, and immunohistochemistry. We also described chemotherapy-induced cytomorphological changes of MBT. Histopathological examination revealed one case with a substantially increased cytologic atypia, including extreme nuclear enlargement, marked nuclear pleomorphism, and multiple, prominent nucleoli. Necrosis or degenerative change was not evident. In contrast, another case displayed large coagulative tumor cell necrosis, hemorrhage, and fibrosis. Irregularly distributed islands, tumor cells in sheets or cords or scattered individually were located adjacent to the necrotic areas. The individual tumor cells showed large, bizarre, degenerative-appearing nuclei with smudged or clumped chromatin. These cells had large amounts of dense, eosinophilic cytoplasm with microvesiculation and macrovesiculation. Experiences with chemotherapy-induced cytomorphological changes of MBT have been limited. This study demonstrated the effect of chemotherapy on MBT cytomorphology. Preoperative chemotherapy is increasingly used to manage ovarian cancer. Therefore, pathologists should be aware of the morphological effects of chemotherapy.

Keywords: Chemotherapy, interval debulking surgery, malignant Brenner tumor, cytology

Introduction

Approximately 70% of ovarian cancers are not diagnosed until the disease involves the upper abdomen or has spread beyond the abdominal cavity [1]. Conventional treatment for advanced ovarian cancer is "optimal" debulking, which is aggressive cytoreductive surgery to remove all macroscopic lesions, and postoperative concurrent chemoradiation therapy, usually consisting of a platinum-containing agent and a taxane, to achieve prolonged progression-free and overall survival [2, 3]. However, this aggressive approach has 5-year overall survival rates of 10-20% in patients with FIGO stage IIIC (the most common stage of ovarian cancer) or IV diseases [4, 5]. For this reason, neoadjuvant chemotherapy was developed as an alternative therapeutic strategy for women with advanced ovarian cancer.

The principle of preoperative chemotherapy is administering chemotherapy before performing cytoreductive surgery [6, 7]. Researchers have reported dramatic clinical responses in patients who were too medically compromised to tolerate primary surgical cytoreduction. Improved diagnostic techniques have enabled clinicians to identify patients with advanced diseases who are unlikely to be optimally resected at initial surgery [7, 8]. Consequently, preoperative chemotherapy has gained popularity as a means of improving the physical and emotional trauma associated with initial ovarian cancer treatment [9].

Table 1. Antibodies used for immunohistochemical staining

Antibody	Source	Clone	Dilution
p63	Dako, Agilent Technologies, Inc., Carpinteria, CA, USA	DAK-p63	1:150
CK5/6	Dako, Agilent Technologies, Inc., Carpinteria, CA, USA	D5/16 B4	1:200
PAX8	Cell Marque Corp., Rocklin, CA, USA	Polyclonal	1:50
WT1	Cell Marque Corp., Rocklin, CA, USA	6F-H2	1:100
p16	Ventana Medical Systems, Inc., Tucson, AZ, USA	E6H4	RTU
p53	NovoCastra Laboratories, Ltd,, Newcastle upon Tyne, UK	DO-7	1:300
ER	Thermo Fisher Scientific Inc., Fremont, CA, USA	SP1	1:100
PR	Dako, Agilent Technologies, Inc., Carpinteria, CA, USA	PgR 636	1:50
CK7	Dako, Agilent Technologies, Inc., Carpinteria, CA, USA	OV-TL 12/30	1:100
CK20	Dako, Agilent Technologies, Inc., Carpinteria, CA, USA	Ks 20.8	1:100
CDX2	Cell Marque Corp., Rocklin, CA, USA	EPR2764Y	1:400

CK5/6: cytokeratin 5/6; PAX8: paired box 8; WT1: Wilms tumor 1; ER: estrogen receptor; PR: progesterone receptor; CK7: cytokeratin 7; CK20: cytokeratin 20; CDX2: caudal type homeobox 2; RTU: ready-to-use.

Neoadjuvant chemotherapy is being used at many institutions for preoperative management of advanced ovarian cancers. Application of chemotherapeutic agents induces obvious cytomorphological changes in the cells of tumor tissues from patients who received chemotherapy. Although the effects of chemotherapy on the cytomorphology of ovarian cancer cells have been reported, to the best of our knowledge, no data are available on chemotherapy-induced alterations in the cytomorphology of ovarian malignant Brenner tumors (MBTs). Little has been reported about cytomorphological changes that may pose diagnostic difficulties in the setting of known primary ovarian cancer. In this study, we summarize cytological and histopathological features of MBTs and describe morphological alterations induced by chemotherapy. Pathologists should be aware of this morphology because preoperative chemotherapy is likely to be used more frequently to manage advanced ovarian cancer.

Patients and methods

Patients and tissue specimens

From the surgical pathology files from 2013 to 2015, 15 patients with Brenner tumors were identified: 4 had MBTs, 2 had borderline Brenner tumors, and 9 had benign Brenner tumors. Two of the four patients with MBT received chemotherapy. Chemotherapy regimens varied among patients, but both received a carboplatin and taxane. For comparison of histopathological features, all slides obtained from the 2 cases of borderline Brenner tumor and the 9 cases of benign Brenner tumor were also reviewed. This study was reviewed and approved by the Institutional Review Board at Severance Hospital (2015-2225-001).

Scraping cytology preparation

Gross examination of biopsied and resected specimens was by thorough inspection and palpation. Specimens were cut with a sharp knife into two or more pieces. If necessary, the cut surface was wiped to remove excess blood. The area thought to be most representative of the lesion was chosen by repeat inspection and was scraped with a sharp scalpel. The resulting semifluid drop was spread on a glass slide in the same manner as that of conventional fine-needle aspiration cytology. Three to four slides from different representative areas were made for each sample. Slides were immediately put into 95% ethyl alcohol and stained with hematoxylin and eosin (H&E) and a modified Papanicolaou stain.

Histopathological examination

After cytology, specimens were fixed in 10% neutral-buffered formalin and embedded in paraffin blocks. From each formalin-fixed, paraffin-embedded (FFPE) block, 4-μm sections were cut and stained with H&E, and prepared for immunohistochemical staining. All slides were examined under routine light microscopy by two independent pathologists.

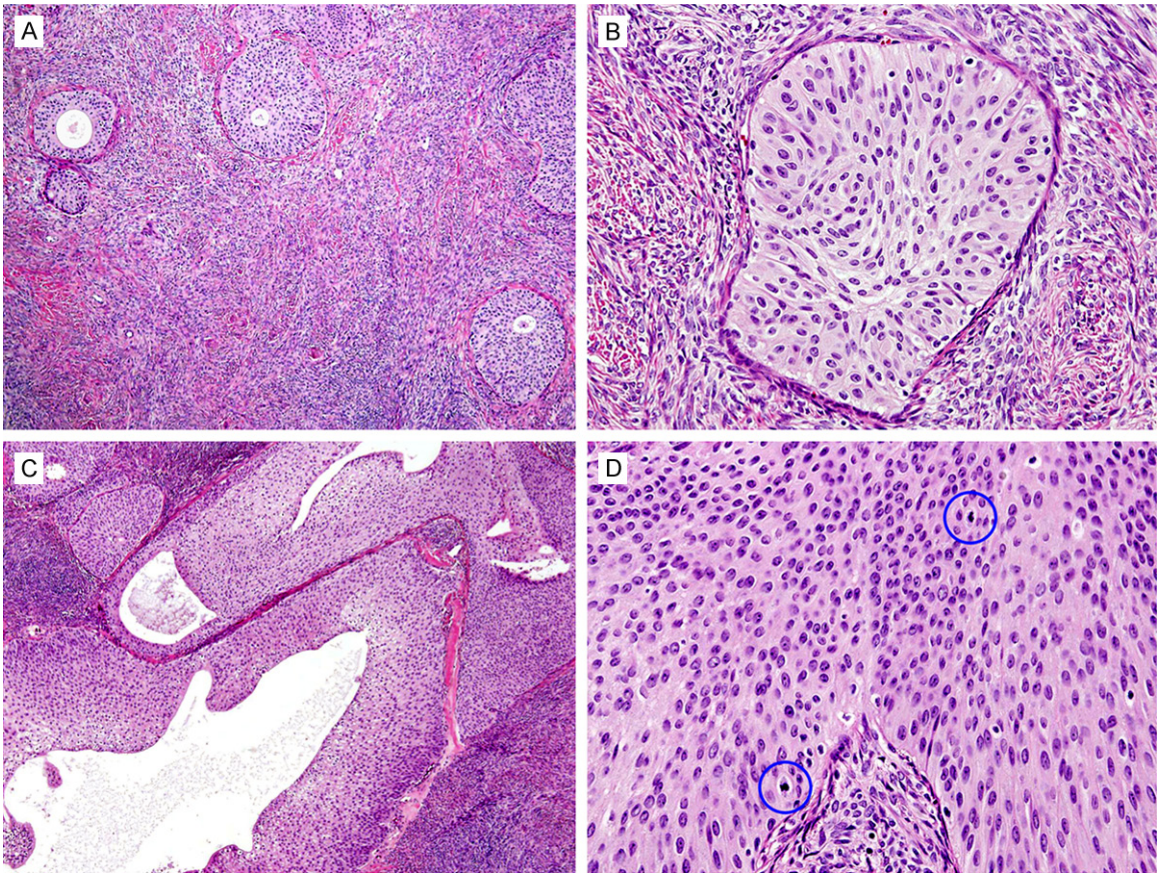

Figure 1. Histopathological findings of benign and borderline Brenner tumors. A. Low-power view of benign Brenner tumor. Well-demarcated nests of tumor cells are shown within dense fibrous stroma. B. High-power view of a benign Brenner tumor. The tumor cells contain round-to-oval nuclei without cytologic atypia. C. Low-power view of a borderline Brenner tumor. The tumor cell nests are characteristically large and cystic, with papillary or polypoid protrusions into cystic spaces and more irregularly shaped than benign Brenner tumors. D. High-power view of a borderline Brenner tumor. Epithelial proliferation was higher for borderline than for benign Brenner tumor. The tumor cells show mild-to-moderate cytologic atypia, with nuclear enlargement and occasional mitotic figures (blue circles).

Immunohistochemistry

FFPE sections were deparaffinized and rehydrated with a xylene and alcohol solution. Immunohistochemical staining used the Ventana Benchmark XT automated staining system (Ventana Medical Systems, Inc., Tucson, AZ, USA) or Dako Omnis (Dako, Agilent Technologies, Inc., Carpinteria, CA, USA) according to the manufacturer's instructions. Antigen retrieval used Cell Conditioning Solution (CC1; Ventana Medical Systems, Inc.) or EnVision FLEX Target Retrieval Solution, High pH (Dako, Agilent Technologies, Inc.). Sections were incubated with primary antibodies (**Table 1**). After chromogenic visualization using ultraView Universal DAB Detection Kit (Ventana Medical Systems, Inc.) or EnVision FLEX/HRP (Dako, Agilent Technologies, Inc.), slides were counterstained with hematoxylin and coverslipped. Appropriate positive and negative controls were stained concurrently to validate staining.

Results

Histopathology of benign and borderline Brenner tumors

Benign Brenner tumors had scattered, small, round-to-polygonal nests of urothelium-like epithelial cells surrounded by dense fibrous stroma (**Figure 1A**). Occasional microcysts appeared within the nests. The tumor cells had sharp outlines with polygonal, pale-to-eosinophilic cytoplasm (**Figure 1B**). The tumor cells were relatively uniform in size with distinct cell borders. The tumor cell nuclei often had longi-

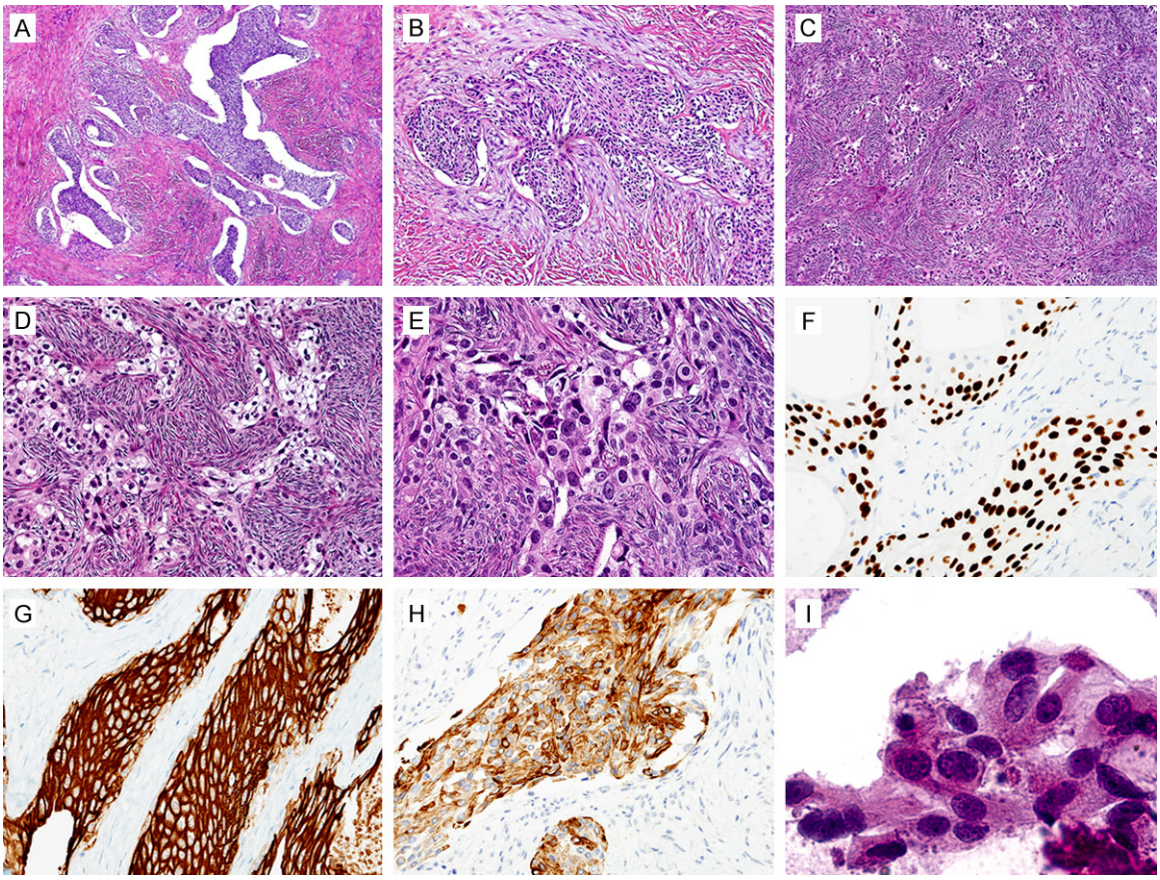

Figure 2. Histopathological, immunohistochemical, and cytological findings of MBT. A. Scanning view of MBT (case 1). Variably sized, irregularly shaped nests of tumor cells are surrounded by dense collagenous stroma. These nests are separated by cleft-like retraction spaces from the stroma. B. Low-power view of MBT (case 1). The tumor cell nests are outlined by irregularly infiltrating borders and an obvious stromal desmoplasia. C. Low-power view of MBT (case 2). The tumor cells are predominantly in irregular or anastomosing cords 2-3 cells thick. D. Medium-power view of MBT (case 2). Irregular-shaped clusters and cords of tumor cells infiltrate the stroma. E. High-power view of MBT (case 2). The tumor cells have distinct borders and pleomorphic nuclei with hyperchromasia and conspicuous nucleoli. The cytoplasm is abundant and clear to eosinophilic. F-H. Immunohistochemical findings. The tumor cells react with F. p63, G. CK7, and H. CK5/6. I. Scraping cytologic preparation of MBT. The tumor cells are loosely aggregated and irregularly distributed. They show abundant eosinophilic cytoplasm and large, hyperchromatic nuclei with coarse chromatin and one or more prominent nucleoli.

tudinal grooves and small, inconspicuous nucleoli. No cytologic atypia or mitotic figures were found.

Borderline Brenner tumors showed several large, irregular-shaped nests of tumor cells, most of which displayed cystic dilatation with intraluminal papillary or polypoid protrusions (**Figure 1C**). The intervening stroma of borderline Brenner tumors was less obvious than for benign Brenner tumors. Prominent nuclear stratification was noted. The degree of epithelial proliferation was higher for borderline than benign Brenner tumors. Although most tumor cells showed mild cytologic atypia, some exhibited moderate atypia with nuclear enlargement and hyperchromasia. Three mitotic figures were detected in 10 high-power fields (**Figure 1D**). The morphological features of borderline Brenner tumors were similar to a low-grade urothelial carcinomas.

Histopathology of MBT

MBT cells were arranged in nests with irregular borders or showed a geographic, anastomosing or jigsaw pattern indicative of an invasive tumor (**Figure 2A**). Variably sized, irregularly shaped tumor cell nests were delineated by infiltrating borders with obvious stromal desmoplasia

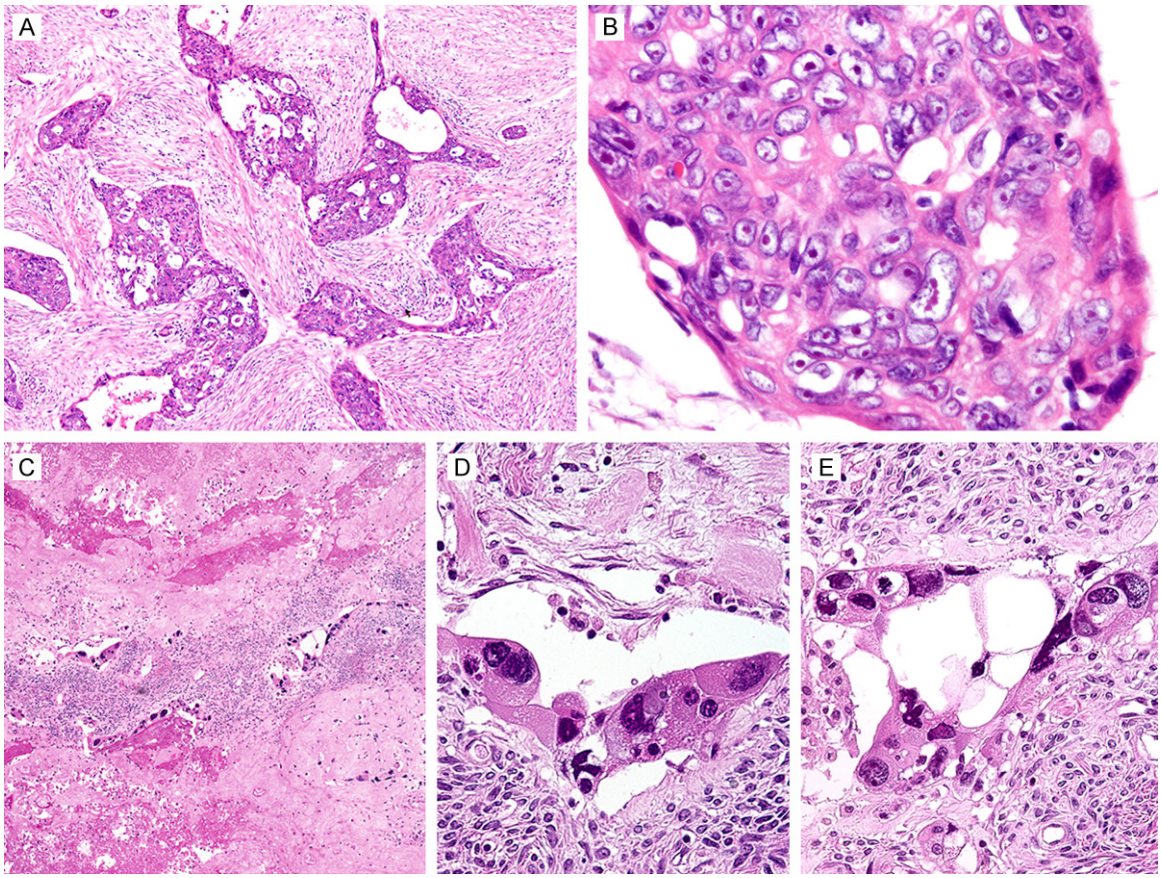

Figure 3. Histopathological and cytological findings of chemotherapy-treated MBT. A. Low-power view of chemotherapy-treated MBT (case 1). Similar to chemotherapy-naive MBTs, the tumor cell nests have jagged contours, infiltrate the stroma, and frequently anastomose. The stroma is densely fibrotic, but does not show necrosis or degeneration. B. High-power view of chemotherapy-treated MBT (case 1). The tumor cells have substantial nuclear atypia. A marked nuclear enlargement, conspicuous, occasionally multiple cherry-red nucleoli, and increased membrane irregularity are observed. Shown is a chromatin clearing with chromatin margination along the membrane. No coagulative tumor cell necrosis or degenerative change is identified. C. Scanning view of chemotherapy-treated MBT (case 2). Compared to Image A, Image C demonstrates large areas of coagulative tumor cell necrosis and hemorrhage. Some scattered clusters and cords of tumor cells (middle one-third) are adjacent to necrosis. D and E. High-power view of chemotherapy-treated MBT (case 2). Large, degenerative-appearing nuclei show coarse or smudged chromatin and a marked irregularity of the nuclear membrane. The tumor cell nuclei are 10-fold larger than surrounding stromal cells. Nucleus-to-cytoplasm ratio was decreased because of increased cell size. The cytoplasm is densely eosinophilic, with microvacuolation. Some tumor cells have large intracytoplasmic vacuoles and perinuclear halo-like appearances. Cyst-like clear spaces are noted between the tumor cells.

(**Figure 2B**). Cleft-like retraction spaces separated tumor nests from stroma. In some areas, the tumor cells with large, hyperchromatic nuclei were arranged predominantly in cords that were 2-3 cells thick (**Figure 2C**). These cells had distinct borders with abundant, eosinophilic cytoplasm (**Figure 2D**). The tumor cell nuclei displayed marked pleomorphism and membrane irregularity (**Figure 2E**). Twelve mitotic figures were observed in 10 high-power fields. Immunohistochemically, the tumor cells were strongly and uniformly positive for p63 (**Figure 2F**), cytokeratin 7 (CK7; **Figure 2G**), and CK5/6 (**Figure 2H**), but negative for PAX8, Wilms tumor 1 (WT1), p16, p53, estrogen receptor (ER), progesterone receptor (PR), CK20, and caudal type homeobox 2 (CDX2). Densely packed, benign-appearing stromal cells were arranged in a whirling or herringbone pattern and had small, ovoid-to-spindle-shaped nuclei.

Cytomorphology of MBT

Scraping cytologic smears were hypercellular, with scattered, irregularly shaped, loosely ar-

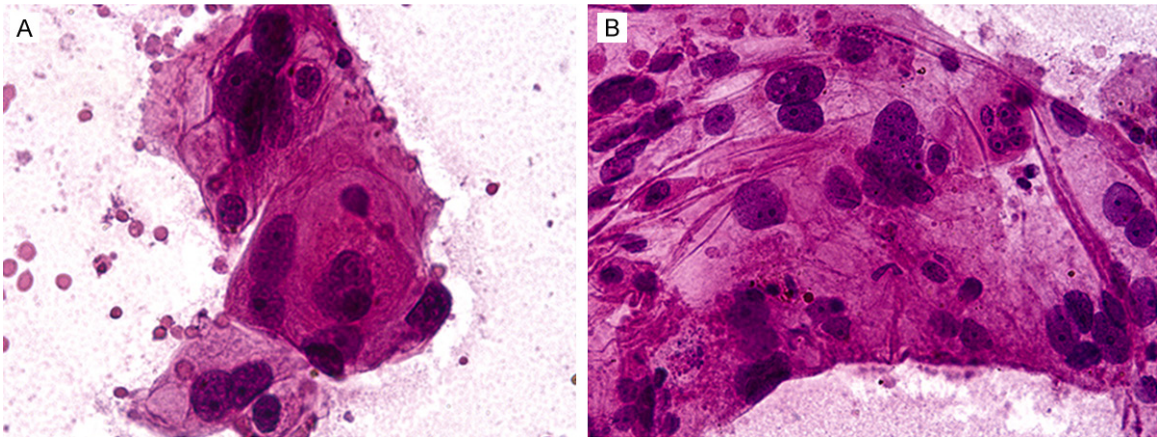

Figure 4. Scraping cytologic preparation of chemotherapy-treated MBT. A. The tumor cells have abundant, densely eosinophilic cytoplasm and large, pleomorphic nuclei. The cell border is relatively distinct. B. Pleomorphic nuclei are randomly distributed through a pool of abundant, densely eosinophilic cytoplasm that appears to be merged with each other. Note a significant variability in nuclear size and shape, accompanied by a low nucleus-to-cytoplasm ratio.

ranged clusters of tumor cells (**Figure 2I**). The tumor cells had relatively distinct cell borders and enlarged, hyperchromatic nuclei. Markedly pleomorphic, bizarre nuclei were occasionally detected. Most tumor cell nuclei showed hyperchromasia, membrane irregularity, and one or more prominent nucleoli. Mitoses were frequently observed. The cytomorphological features were consistent with those observed in MBT tissue sections.

Histopathology of chemotherapy-treated MBT

We could examine two cases of chemotherapy-treated MBT. In both cases, chemotherapy-treated MBTs exhibited distinctive morphological characteristics when compared with MBTs of the patients who did not receive chemotherapy (chemotherapy-naive MBTs). Furthermore, there were obvious morphological differences between the two cases. Firstly, in case 1, low-power views of chemotherapy-treated MBTs were similar to chemotherapy-naive MBTs, with the tumor cell nests in irregular, jagged arrangements surrounded by desmoplastic stroma and retraction artifacts surrounding the nests (**Figure 3A**). By high-power views, the nuclei of chemotherapy-treated MBT cells were larger and had irregular nuclear membranes compared to chemotherapy-naive MBTs. Obvious nuclear clearing with margination of chromatin along the nuclear membrane and multiple, prominent, cherry-red nucleoli were noted (**Figure 3B**). Mitotic figures were often observed, including a few atypical mitoses. The cytoplasm was either intensely eosinophilic or clear, with variably sized vacuoles. No coagulative tumor cell necrosis, hemorrhage, cholesterol clefts, fibrinous debris, or nuclear degenerative change was detected. The stroma showed a diffuse desmoplastic response, with moderate inflammatory infiltrate. Fine collagen fibrils were occasionally admixed with reactive fibroblast-like cells. No thick collagen bundles or hyalinized fibrotic reactions were observed.

Secondly, in case 2, large areas of coagulative tumor cell necrosis and hemorrhage were evident. Cords or clusters of surviving tumor cells were scattered and adjacent to necrotic areas (**Figure 3C**). Individual tumor cells had both nuclear and cytoplasmic alterations. Nuclear features included extreme enlargement with irregular outlines. In a few areas, the tumor cell nuclei were more than 10-fold larger than adjacent stromal cells (**Figure 3D**). Sometimes, the nuclei had such a bizarre outline that they mimicked multinucleated giant cells. Moreover, they appeared degenerated, with chromatin clumping or smudging. The cytoplasm was abundant and intensely eosinophilic. Aggregates of intracytoplasmic microvesicles resulted in a foamy appearance (**Figure 3D**). Some tumor cells had large intracytoplasmic vacuoles, resembling perinuclear haloes. Cyst-like spaces were observed between individual tumor cells (**Figure 3E**). Mitotic figures were rarely detected. The stroma was often densely fibrotic

and contained inflammatory cells, cholesterol clefts, and fibrinous debris.

Immunohistochemically, no significant change in the expression pattern was observed after chemotherapy. In both cases, the tumor cells were positive for p63, CK7, and CK5/6, but negative for PAX8, WT1, p16, p53, ER, PR, CK20, and CDX2.

Cytomorphology of chemotherapy-treated MBT

Scraping cytologic preparation showed moderately cellular smears, with necrotic and hemorrhagic backgrounds. Several irregularly shaped cell clusters had large atypical cells with relatively distinct cell borders and pleomorphic nuclei with coarse chromatin and conspicuous nucleoli (**Figure 4A**). Mitoses were infrequent. Abundant, dense eosinophilic cytoplasm merged to form cytoplasmic pools (**Figure 4B**). Despite the nuclear enlargement, the increase in cytoplasm resulted in a low nucleus-to-cytoplasm ratio. These cytomorphological features were consistent with tissue sections from chemotherapy-treated MBTs.

Discussion

Preoperative chemotherapy is used to treat several cancers, including breast, lung, stomach, and colorectal cancer [10-14]. Because of dramatic response rates to chemotherapy, interval debulking surgery after chemotherapy is also increasingly used to treat advanced ovarian cancers. Although some studies reported the effects of preoperative chemotherapy on cellular morphology [10, 15-19], few studies have investigated morphological changes in chemotherapy-treated ovarian cancer. Three previous reports documented the morphological effects of chemotherapy on ovarian cancer [15, 20, 21]. Chew and colleagues [15] reported that the cytomorphological alterations in ovarian cancer paralleled changes in cancers of other organs. They observed significant alterations in both nuclei (enlargement with membrane irregularities, chromatin smudging and clumping, and overall degenerative appearance) and cytoplasm (clear-to-foamy change due to microvesiculation and macrovesiculation, eosinophilia, and granularity). McCluggage and colleagues [20] also found that the morphological effects of chemotherapy on ovarian cancer are characterized by both nucleus (enlargement with extremely bizarre nuclear outlines and smudged or clumped chromatin) and cytoplasm (eosinophilia or clear cell change with a vacuolated or foamy appearance) Wang and colleagues [21] observed extensive tumor necrosis and surviving tumor cells in a background of fibrosis. The tumor cells that were individually scattered or arranged in cords and islands were approximately 3-4 times larger than non-enlarged tumor cells and had large amounts of eosinophilic cytoplasm with vacuoles. These observations indicate that histological grading of tumors, which has important prognostic implications and depends on the assessment of both cytological and architectural features, is not reliable after chemotherapy [20]. In addition, in tumors that respond well to chemotherapy, surviving cells with a clear, vacuolated cytoplasm may exist as individually scattered cells or small clusters of cells within a fibrotic stroma or areas of necrosis. These cells may be difficult to identify and, accordingly, missed or misinterpreted as histiocytes. In this study, we investigated the effects of chemotherapy on the cytomorphology of ovarian MBTs. To the best of our knowledge, chemotherapy-induced morphological alterations of MBT have not been documented. The morphological features we observed for MBTs treated with chemotherapy were similar to previous studies. Microscopically, one case revealed a substantially increased cytologic atypia including nuclear enlargement, marked nuclear pleomorphism, and multiple, prominent nucleoli. No necrosis or degenerative change was observed. In contrast, another case had large coagulative tumor cell necrosis, hemorrhage, and fibrosis. The tumor cells in irregularly distributed islands, sheets or cords of tumor cells or individually scattered were located adjacent to necrotic areas. Individual tumor cells had large, bizarre, and degenerative-appearing nuclei with smudged or clumped chromatin. They had large amount of dense, eosinophilic cytoplasm with vesicles. Taken together, these results showed that careful morphological examination with or without the aid of ancillary techniques should help pathologists determine features that result from chemotherapy.

We further investigated cytomorphology of chemotherapy-treated MBTs using scraping cytologic preparations. Despite the wide application of chemotherapy in cancer treatment, only

a few studies have investigated chemotherapy-induced changes in cytological features using cytologic specimens. In a study by Albright and colleagues [22], radiation-treated lung cancer specimens had significantly decreased cellularity, nuclear and cytoplasmic enlargement, nuclear pyknosis and karyorrhexis, blurring of nuclear chromatin, and cytoplasmic vacuolation. These alterations are similar to changes observed in tissue samples of other chemotherapy-treated malignancies. A significant decrease in the number of viable tumor cells after chemotherapy may create diagnostic challenges because of false-negative results for cytologic specimens from patients who received chemotherapy. A few studies compared the sensitivity and specificity for frozen sections and touch-imprint cytology of sentinel lymph nodes from breast cancer patients [23-26]. No significant differences were observed in sensitivity and specificity between the two modalities except for micrometastasis. Chemotherapy did not affect the diagnostic accuracy of touch-imprint cytologic preparations [24]. Thus, assuming that the morphological features of cytologic smears closely reflect histological appearances is reasonable. In this study, we observed substantial changes in the cytological characteristics of MBTs using scraping cytologic smears. We observed several clusters of tumor cells scattered in a necrotic background with markedly pleomorphic nuclei, coarse chromatin, and conspicuous nucleoli. Abundant eosinophilic cytoplasm merged to create cytoplasmic pools. A concomitant increase in the amount of nucleus and cytoplasm resulted in a low nucleus-to-cytoplasm ratio. These cytomorphological features were consistent with observations of tissue sections.

The histopathological and cytological features induced by chemotherapy might be considered in differential diagnoses. First, extensive coagulative tumor cell necrosis and a relatively small amount of residual tumor tissue observed in ovaries raises the concern of metastatic carcinoma from the gastrointestinal tract. Metastatic tumor tissue from the gastrointestinal tract typically shows variable amount of cytoplasmic mucin, most primary ovarian cancers do not contain mucin. Furthermore, metastatic tumor cells from the gastrointestinal tract do not usually have bizarre, hyperchromatic nuclei and large amount of vacuolated cytoplasm. In contrast, these cytologic features were characteristic of chemotherapy-treated ovarian cancers. In those cases, immunohistochemistry was useful for confirming the histopathological diagnosis. The most useful panels are p63, CK5/6, CK7, CK20, CDX2, PAX8, WT1, p53, p16, ER, and PR. Ovarian MBTs are positive for p63, CK5/6, and CK7. Ovarian high-grade serous carcinomas are positive for PAX8, WT1, ER, p53, and p16. In contrast, both MBTs and high-grade serous carcinomas are negative for CK20 and CDX2. The reverse is true for gastrointestinal carcinomas. In particular, colorectal carcinomas are strongly and uniformly positive for CK20 and CDX2, but negative for PAX8, WT1, ER, and PR. Second, abundant, vacuolated cytoplasm in tumor cells suggests clear cell carcinoma. Based on both previous data and our observations, high-grade serous carcinomas and MBTs showed variations in the amount of cytoplasmic vacuoles or clear cytoplasm after chemotherapy [21]. Comparison with pre-chemotherapy findings may readily resolve this issue. Immunoreactivity for p63 and CK5/6 can differentiate MBT from clear cell carcinoma. MBT cells diffuse, strong expression for both p63 and CK5/6, but clear cell carcinoma neither reacts with p63 nor CK5/6. Similarly, WT1 and p53 are reliable biomarkers for differentiating clear cell carcinoma from high-grade serous carcinoma. Clear cell carcinoma cells have no WT1 expression and patchy p53 expression, while high-grade serous carcinomas usually have diffusely positive WT1 and p53 staining.

In conclusion, this study investigated the morphological alterations of chemotherapy-treated MBTs using tissue and cytologic specimens. The samples showed morphological alternations to that were similar to observations from other types of chemotherapy-treated malignancies. Cytomorphological features of chemotherapy-treated MBTs observed in scraping cytologic preparations were consistent with the tissue sections. As preoperative chemotherapy is increasingly used to treat advanced ovarian cancer, pathologists should recognize the associated morphological changes, which may create diagnostic challenges for determining histologic type and grade and identifying residual malignancy. A thorough gross and microscopic examination of post-chemotherapy tumor specimens is required with ample sectioning to

identify small amounts of residual, viable tumor cells.

Acknowledgements

This study was supported by a faculty research grant of Yonsei University College of Medicine for 2016 (6-2016-0130).

Disclosure of conflict of interest

None.

Address correspondence to: Dr. Hyun-Soo Kim, Department of Pathology, Severance Hospital, Yonsei University College of Medicine, 50-1, Yonsei-ro, Seodaemun-gu, Seoul 03722, Republic of Korea. Tel: +82-2-2228-1794; Fax: +82-2-362-0860; E-mail: hyunsookim@yuhs.ac

References

[1] Cannistra SA. Cancer of the ovary. N Engl J Med 1993; 329: 1550-1559.

[2] McGuire WP, Hoskins WJ, Brady MF, Kucera PR, Partridge EE, Look KY, Clarke-Pearson DL and Davidson M. Cyclophosphamide and cisplatin compared with paclitaxel and cisplatin in patients with stage III and stage IV ovarian cancer. N Engl J Med 1996; 334: 1-6.

[3] Hoskins WJ. Surgical staging and cytoreductive surgery of epithelial ovarian cancer. Cancer 1993; 71: 1534-1540.

[4] Hoskins WJ, Bundy BN, Thigpen JT and Omura GA. The influence of cytoreductive surgery on recurrence-free interval and survival in small-volume stage III epithelial ovarian cancer: a Gynecologic Oncology Group study. Gynecol Oncol 1992; 47: 159-166.

[5] Harries M and Gore M. Part I: chemotherapy for epithelial ovarian cancer-treatment at first diagnosis. Lancet Oncol 2002; 3: 529-536.

[6] Schwartz PE, Chambers JT and Makuch R. Neoadjuvant chemotherapy for advanced ovarian cancer. Gynecol Oncol 1994; 53: 33-37.

[7] Schwartz PE, Rutherford TJ, Chambers JT, Kohorn EI and Thiel RP. Neoadjuvant chemotherapy for advanced ovarian cancer: long-term survival. Gynecol Oncol 1999; 72: 93-99.

[8] Nelson BE, Rosenfield AT and Schwartz PE. Preoperative abdominopelvic computed tomographic prediction of optimal cytoreduction in epithelial ovarian carcinoma. J Clin Oncol 1993; 11: 166-172.

[9] Taylor KJ and Schwartz PE. Cancer screening in a high risk population: a clinical trial. Ultrasound Med Biol 2001; 27: 461-466.

[10] Carder P. Typing breast cancer following primary chemotherapy. Histopathology 1999; 35: 584-585.

[11] Xu AM, Huang L, Liu W, Gao S, Han WX and Wei ZJ. Neoadjuvant chemotherapy followed by surgery versus surgery alone for gastric carcinoma: systematic review and meta-analysis of randomized controlled trials. PLoS One 2014; 9: e86941.

[12] Yu W. A review of adjuvant therapy for resected primary gastric cancer with an update on Taegu's phase III trial with intraperitoneal chemotherapy. Eur J Surg Oncol 2006; 32: 655-660.

[13] Ragnhammar P, Hafstrom L, Nygren P and Glimelius B. A systematic overview of chemotherapy effects in colorectal cancer. Acta Oncol 2001; 40: 282-308.

[14] Lee HC, Lee JO and A. PI. Changes in protein expression in breast cancer after anthracycline-based chemotherapy. Korean J Pathol 2007; 41: 165-170.

[15] Chew I, Soslow RA and Park KJ. Morphologic changes in ovarian carcinoma after neoadjuvant chemotherapy: report of a case showing extensive clear cell changes mimicking clear cell carcinoma. Int J Gynecol Pathol 2009; 28: 442-446.

[16] Sethi D, Sen R, Parshad S, Khetarpal S, Garg M and Sen J. Histopathologic changes following neoadjuvant chemotherapy in various malignancies. Int J Appl Basic Med Res 2012; 2: 111-116.

[17] Kennedy S, Merino MJ, Swain SM and Lippman ME. The effects of hormonal and chemotherapy on tumoral and nonneoplastic breast tissue. Hum Pathol 1990; 21: 192-198.

[18] Becker K, Mueller JD, Schulmacher C, Ott K, Fink U, Busch R, Bottcher K, Siewert JR and Hofler H. Histomorphology and grading of regression in gastric carcinoma treated with neoadjuvant chemotherapy. Cancer 2003; 98: 1521-1530.

[19] Shia J, Guillem JG, Moore HG, Tickoo SK, Qin J, Ruo L, Suriawinata A, Paty PB, Minsky BD, Weiser MR, Temple LK, Wong WD and Klimstra DS. Patterns of morphologic alteration in residual rectal carcinoma following preoperative chemoradiation and their association with long-term outcome. Am J Surg Pathol 2004; 28: 215-223.

[20] McCluggage WG, Lyness RW, Atkinson RJ, Dobbs SP, Harley I, McClelland HR and Price JH. Morphological effects of chemotherapy on ovarian carcinoma. J Clin Pathol 2002; 55: 27-31.

[21] Wang Y and Zheng W. Cytologic changes of ovarian epithelial cancer induced by neoadjuvant chemotherapy. Int J Clin Exp Pathol 2013; 6: 2121-2128.

[22] Albright CD and Hafiz MA. Cytomorphologic changes in split-course radiation-treated bronchogenic carcinomas. Diagn Cytopathol 1988; 4: 9-13.
[23] Jain P, Kumar R, Anand M, Asthana S, Deo SV, Gupta R, Bhutani M, Karak AK and Shukla NK. Touch imprint cytology of axillary lymph nodes after neoadjuvant chemotherapy in patients with breast carcinoma. Cancer 2003; 99: 346-351.
[24] Gimbergues P, Dauplat MM, Durando X, Abrial C, Le Bouedec G, Mouret-Reynier MA, Cachin F, Kwiatkowski F, Tchirkov A, Dauplat J and Penault-Llorca F. Intraoperative imprint cytology examination of sentinel lymph nodes after neoadjuvant chemotherapy in breast cancer patients. Ann Surg Oncol 2010; 17: 2132-2137.
[25] Komenaka IK, Torabi R, Nair G, Jayaram L, Hsu CH, Bouton ME, Dave H and Hobohm D. Intraoperative touch imprint and frozen section analysis of sentinel lymph nodes after neoadjuvant chemotherapy for breast cancer. Ann Surg 2010; 251: 319-322.
[26] Yagata H, Yamauchi H, Tsugawa K, Hayashi N, Yoshida A, Kajiura Y, In R, Matsuda N and Nakamura S. Sentinel node biopsy after neoadjuvant chemotherapy in cytologically proven node-positive breast cancer. Clin Breast Cancer 2013; 13: 471-477.